

# SOS Gate Capacitance Modeling

H. C. Morris\*, E. C. Cumberbatch\*\* and H. Abebe\*\*\*

\*San Jose State University, San Jose, CA, USA, hedleymorris@yahoo.com

\*\*Claremont Graduate University, Claremont, CA, USA, ellis.cumberbatch@cg.edu

\*\*\*MOSIS Service, USC Information Sciences Institute, Marina del Rey, CA, USA, abebeh@mosis.org

## ABSTRACT

A model for the gate capacitance model for the SOS structure is presented. Exact analytic formula and numerical simulations are presented. Both the forward and inverse problems are solved and compared with experimental data.

**Keywords:** Provide up to five keywords to be used for on-line publication searches and indexing.

## 1 INTRODUCTION

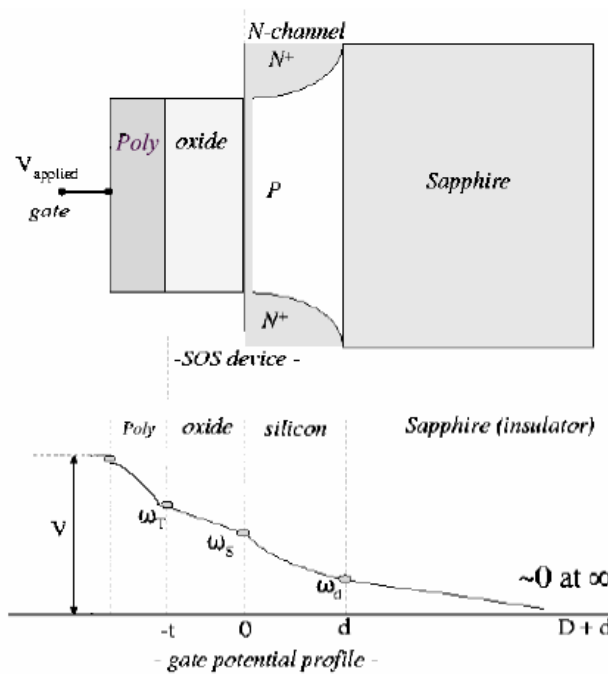


Figure 1: A schematic of a poly SOS device

### 1.1 Basic Equations

The drift-diffusion expressions for electron and hole currents are given by [1]

$$\mathbf{J}_n = q_e (n \mu_n \mathbf{E} + D_n \nabla n) \quad (1.1)$$

$$\mathbf{J}_p = q_e (p \mu_p \mathbf{E} - D_p \nabla p) \quad (1.2)$$

where mobilities  $\mu_n$  and  $\mu_p$  usually depend on doping levels and on  $\mathbf{E}$ , but usually are taken as constant. Using the Einstein relation,

$$D = \frac{kT\mu}{q_e} \quad (1.3)$$

and with  $E = -\nabla \psi$ , we can write these expressions in the following form:

$$\mathbf{J}_n = n \mu_n \nabla (-\psi q_e + kT \log n) = -q_e n \mu_n \nabla \Phi_n \quad (1.4)$$

$$\mathbf{J}_p = -p \mu_p \nabla (\psi q_e + kT \log p) = q_e p \mu_p \nabla \Phi_p \quad (1.5)$$

where  $\Phi_n$  and  $\Phi_p$  are the “quasi-Fermi potentials” for electrons and holes, respectively. The charge density for electrons and holes may be derived now as

$$n = n_i \exp \left[ \frac{q_e}{kT} (\psi - \Phi_n) \right] \quad (1.6)$$

and

$$p = p_i \exp \left[ -\frac{q_e}{kT} (\psi - \Phi_p) \right] \quad (1.7)$$

where  $n_i$  is a constant (dependent on the temperature) called the intrinsic carrier density. (It is the density in the undoped silicon.) Note that

$$np = n_i^2 \exp \left[ \frac{q_e}{kT} (\Phi_p - \Phi_n) \right] \quad (1.8)$$

Gauss' equation and the conservation equations for electrons and hole are:

$$\epsilon \nabla \cdot \mathbf{E} = -\epsilon \nabla^2 \psi = \rho = q_e (p - n + N) \quad (1.9)$$

$$\frac{\partial n}{\partial t} - \frac{1}{q_e} \nabla \cdot \mathbf{J}_n = G_n - U_n \quad (1.10)$$

$$\frac{\partial p}{\partial t} - \frac{1}{q_e} \nabla \cdot \mathbf{J}_p = G_p - U_p \quad (1.11)$$

The above equations constitute three nonlinear partial differential equations for the potentials  $\psi$ ,  $\Phi_n$ , and  $\Phi_p$ .

### 1.2 Boundary Conditions

There is no current flow in the  $x$ -direction perpendicular to the gate since there is no current flow due to the insulating barriers. Thus  $\mathbf{J}_n$  and  $\mathbf{J}_p$  are both zero, and (1.4) and (1.5) imply that  $\Phi_n$  and  $\Phi_p$  are constant in the silicon.

We choose values for  $\Phi_n$  and  $\Phi_p$  so that  $\psi = 0$  in the

silicon at flat-band. Values for  $\Phi_n$  and  $\Phi_p$  at the gate exceed those in the silicon by  $V = V_{app} - V_{FB}$  where  $V_{app}$  is the applied voltage and  $V_{FB}$  is the flat-band voltage. The latter is a sum of the built-in voltage plus voltages due to work function differences across Si/SiO<sub>2</sub> interfaces.  $V_{FB}$  is device dependent and must be specified for each device under consideration.

At the Si/SiO<sub>2</sub> interfaces the boundary conditions are the continuity of electrostatic potential and electric displacement. The latter is stated as

$$\varepsilon \frac{\partial \psi}{\partial x_1}|_{Si} = \varepsilon \frac{\partial \psi}{\partial x_1}|_{SiO_2} \quad (1.12)$$

### 1.3 Scaled Variables

Adopting scaled variables provides transparency to the size of the various terms and indicates the importance of the physical processes that the terms represent. Here, scaling is done in the following way [2, 3]:

$$\lambda = \max \left| \frac{N(x_1)}{n_i} \right|, V_{th} = \frac{kT}{q_e} \\ (\psi, \Phi_n, \Phi_p, V) = (\omega, \phi_n, \phi_p, v) V_{th} \ln \lambda \quad (1.13)$$

$$x_1 = x L_D \left( \frac{\ln \lambda}{\lambda} \right)^{1/2}, C = \varepsilon_{Si} A \frac{1}{L_D (\ln \lambda / \lambda)^{1/2}} c \\ L_D = \left( \frac{kT \varepsilon_{Si}}{n_i q^2} \right)^{1/2}$$

The lengths  $t_{ox}$ ,  $d_1$  and  $D_1$  are scaled to  $t$ ,  $d$ , and  $D$ , respectively. Applying this scale to the charge conservation equation results in a second-order differential equation for the spatial potential  $\omega(x)$ .

### 1.4 Metal Gate

This is a one-dimensional problem since we take only  $x$  dependence into consideration. The scaling and the substitution of variables into the Gauss' equation give:

$$\omega'' = e^{(\omega-1-\phi_n) \ln \lambda} - e^{-(\omega+1-\phi_p) \ln \lambda} + 1, 0 < x < d. \quad (1.14)$$

The scaled quasi-Fermi potentials are chosen to equal 1 in  $0 < x < d$ , yielding

$$\omega'' = e^{(\omega-2) \ln \lambda} - e^{-\omega \ln \lambda} + 1, \quad 0 < x < d. \quad (1.15)$$

The boundary conditions on  $\omega$  are

$$\omega = \begin{cases} 0 & \text{at } x = d + D \\ v & \text{at } x = -t \end{cases} \quad (1.16)$$

$\omega$  is continuous at  $x = 0$  and at  $x = d$  and at these interfaces

$$\omega'_S = r(\omega_S - v) \quad \text{where} \quad r = \varepsilon_{ox} / t \varepsilon_{Si} \\ \omega'_d = -r_D \omega_d \quad \text{where} \quad r_D = \varepsilon_{ox} / D \varepsilon_{Si} \quad (1.17)$$

In the above the subscript  $S$  refers to  $x = 0$  and the subscript  $d$  refers to  $x = d$ . In the derivation of the latter two boundary conditions we have used  $\omega'' = 0$  in the two oxides, so that the potentials are linear there. We require the relationship  $\omega'_S(v)$  so that we can determine the capacitance

$$c = -\frac{d\omega'_S}{dv}. \quad (1.18)$$

The following subsections of section 3 are concerned with solutions to these equations in various regimes (depletion, flat-band, inversion, accumulation) and attempts at an overall numerical solution.

### 1.5 Poly Gate

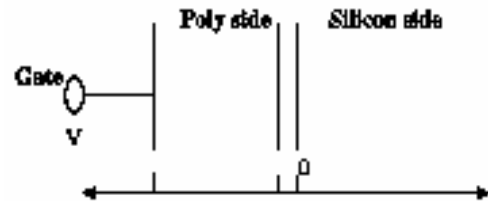


Figure 2.A schematic of the poly gate

The SOS device that uses poly gate differs from the one that uses metal gate in that the voltage is no longer constant through the gate as it is in the metal case. Instead, the potential drops in a parabolic fashion until it encounters the insulator at  $x = -t$ . We let  $\omega_T$  denote the potential at  $x = -t$  and let  $x_n$  denote the thickness of the poly layer. Adjusting the full equations accordingly, we have the basic equations for the poly gate case:

$$F(\omega) = 2\varepsilon e^{(\omega-2)/\varepsilon} + 2\omega \quad (1.19)$$

$$F(\omega_S) - r_f^2 (\omega_S - \omega_T)^2 = F(\omega_d) - r_b^2 \omega_b^2 \quad (1.20)$$

$$\omega'_S = r_f (\omega_S - \omega_T) \quad (1.21)$$

$$\omega'_d = -r_b \omega_d \quad (1.22)$$

$$\int_{\xi}^{\zeta} \frac{d\zeta}{\sqrt{F(\zeta + \omega_d) - F(\omega_d) + r_b^2 \omega_d^2}} = d \quad (1.23a)$$

$$\omega_S = \xi + \omega_d \quad (1.23b)$$

$$\omega_T = v - \frac{\beta}{2} \omega'_S \quad (1.24)$$

The equations (1.19)-(1.24) describe the potential  $\omega$  inside the poly gate device. From (1.20) and (1.21) we have

$$\omega_T = \omega_S + \frac{1}{r_f} \sqrt{F(\omega_S) - F(\omega_d) + r_b^2 \omega_d^2} \quad (1.25)$$

which defines  $\omega_T$  in terms of  $\omega_d$ . From (1.21) and (1.24) the voltage  $v$  is given by

$$v = \omega_T + \frac{\beta}{2} r_f^2 (\omega_S - \omega_T)^2 \quad (1.26)$$

To solve the equations (1.19)-(1.24) we adapt the following strategy:

- For each  $\omega_d$  solve (1.24) for  $\omega_S$ .
- From (1.25) obtain the effective gate voltage  $\omega_T$ .
- Use (1.26) to relate  $\omega_T$  to  $v$ .

This process defines the voltage  $v$  as a function of  $\omega_d$ .

Equation (1.25) can be inverted to give  $\omega_T$  in terms of  $v$  and  $\omega_S$  by the following formula.

$$\omega_T = \omega_S + \frac{1}{\beta r_f^2} \left( \sqrt{1 + 2\beta r_f^2(v - \omega_S)} - 1 \right) \quad (1.27)$$

## 2 APPROXIMATE SOLUTIONS

We have constructed two asymptotic solutions [4] to equation (1.23a) based on the parameter  $\delta = e^{-(\omega_d-2)/2\varepsilon}$ .

The solution

$$\xi_L(\omega_d) = \varepsilon(1+\delta^2) \left( \cosh\left(\frac{d}{\sqrt{\varepsilon}\delta}\right) - 1 \right) + r_b \omega_d \sqrt{\varepsilon} \delta \sinh\left(\frac{d}{\sqrt{\varepsilon}\delta}\right) \quad (2.1)$$

is valid for  $\omega_d < 2$  ( $\delta \rightarrow \infty$ ), and the solution

$$\xi_U(\omega_d) = 2\varepsilon \ln(\sec(\frac{1}{\sqrt{2\varepsilon}} de^{(\omega_d-2)/2\varepsilon})) \quad (2.2)$$

is valid for  $\omega_d > 2$  ( $\delta \rightarrow 0$ ). When  $\omega_d < 2$  the parameter  $\delta$  is large and becomes essentially infinite as  $\omega_d \rightarrow 0$ . For  $\omega_d > 2$ , the parameter  $\delta$  is small and

tends to zero as  $\omega_d \rightarrow \omega_d^\infty = 2 + 2\varepsilon \ln \frac{\pi}{d} \sqrt{\frac{\varepsilon}{2}}$ . For

$\delta > 1$  the function  $\xi_L(\omega_d)$  has the asymptotic form

$$\xi_L \approx dr_b \omega_d + \frac{1}{2} d^2 (1 + \delta^{-2}) \quad (2.3)$$

while, for  $\delta < 1$ , the function  $\xi_U(\omega_d)$  has the asymptotic form

$$\xi_U(\omega_d) \approx \frac{1}{2} d^2 \delta^{-2} \quad (2.4)$$

Equations (2.3) and (2.4) suggest the composite, or blended, formula

$$\xi_B(\omega_d) = dr_b \omega_d + \frac{1}{2} d^2 + 2\varepsilon \ln(\sec(\frac{1}{\sqrt{2\varepsilon}} de^{(\omega_d-2)/2\varepsilon})) \quad (2.5)$$

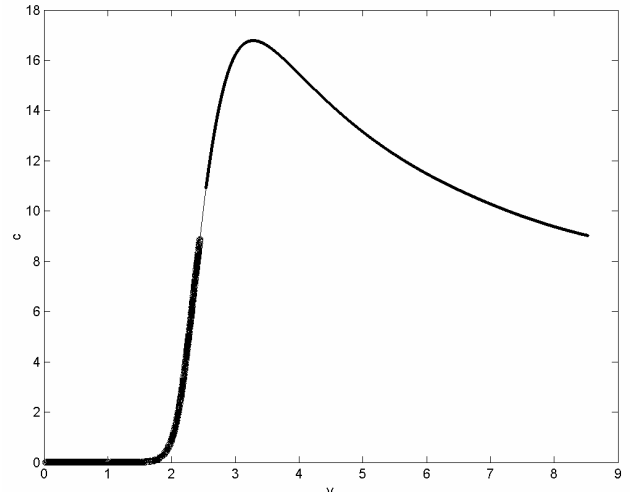


Figure 3. The approximate solutions (2.1), (2.2) and (2.5).

The lower curve in Figure 3 is the solution (2.1) and the upper curve is the solution (2.2). The thin curve is the blended solution (2.5) that joins them over the complete voltage range. All variables are scaled.

## 3 THE INVERSE PROBLEM

Figure 4 shows a measured capacitance-voltage curve for an SOS N Gate device.

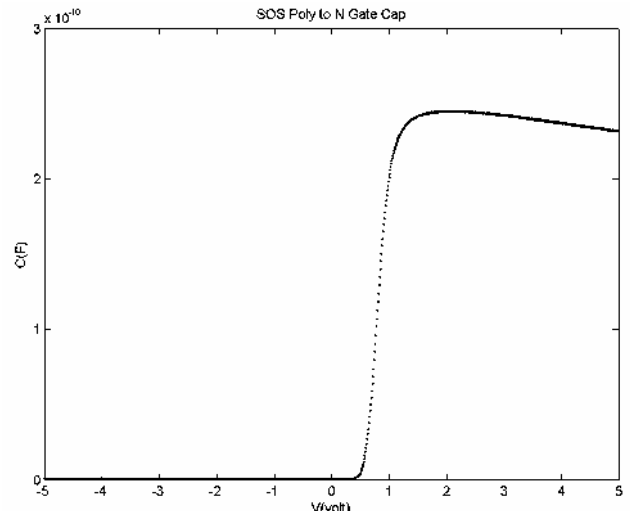


Figure 4: A capacitance curve for a Poly to N device

Equation (2.5) provides a model for the capacitance-voltage relationship in the SOS Poly Gate device. This model can now be used to solve the inverse problem of finding the device parameters. Specifically, we seek the thicknesses of the silicon layer, the oxide layer and the sapphire layer.

### 3.1 The Algorithm

The inverse algorithm follows the algorithm below:

- Set the initial guess of eight parameters (thicknesses of silicon ( $d$ ), oxide ( $t$ ), and sapphire ( $D$ ) layers,  $r_b$ ,  $r_f$ ,  $V_{FB}$ , and  $\beta$ ).
- Fit the model data from the blended approximation curve from (2.5) to the data.
- Repeat until the model data fit the measured data within a suitable tolerance.
- Output the parameters: Silicon layer thickness, oxide layer thickness, sapphire layer thickness.

### 3.2 Results

A Levenberg-Marquardt optimization technique was used to find the optimal parameter values. To ensure that the algorithm was effective we first tested it on simulated data. Figure 5 show a typical fit. The parameter optimal parameter values were in excellent agreement with the known values.

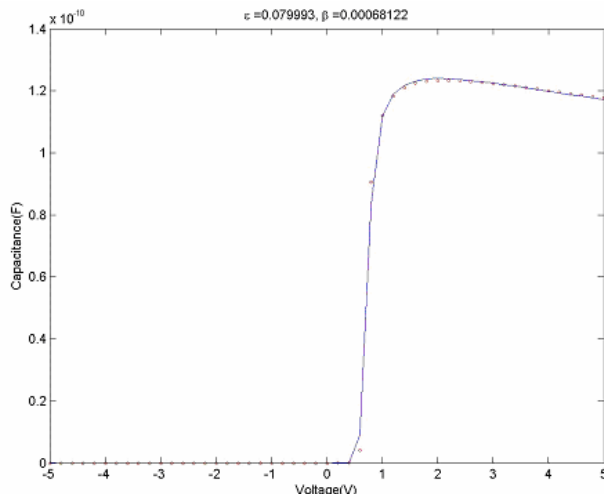


Figure 5: A fit to the capacitance vs. voltage curve for simulated data. The circles are the simulated points and the solid line is the fit from the model.

Figure 6 shows the result of a fit to measured data. The fit is excellent and the parameter values identified were physically realistic.

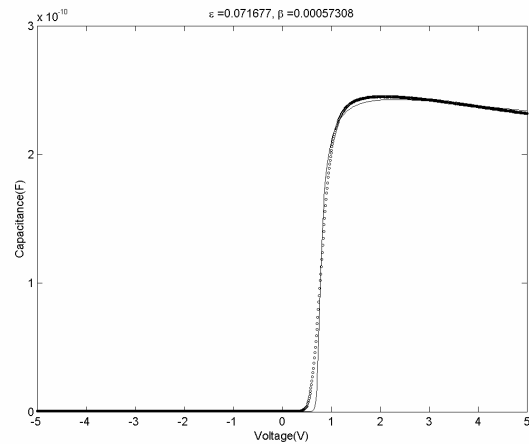


Figure 6: A fit to the capacitance vs. voltage curve for real data. The dots are the experimentally measured points and the solid line is the fit from the model.

### ACKNOWLEDGMENTS

This work was supported by MOSIS, Information Sciences Institute, University of Southern California

### REFERENCES

- [1] P.A. Markowich, C.A. Ringhofer, and C. Schmeiser, "Semiconductor Equations," Wien, New York: Springer-Verlag, 1990.
- [2] M. Ward *et al*, "Asymptotic methods for metal oxide semiconductor field effect transistor modeling," *SIAM J Appl. Math*, vol. 50, No. 4, pp. 1099-1125, Aug 1990.
- [3] E. Cumberbatch, H. Abebe, and H. Morris, "Current-voltage characteristics from an asymptotic analysis of the MOSFET equations," *J. of Engineering Mathematics*, vol. 39, pp. 25-46, 2001.
- [4] J. Kevorkian and J. D. Cole, 'Multiple Scale and Singular Perturbation Methods', Springer-Verlag, 1996 San Francisco, CA, USA.